Simultaneous heat and moisture transport in porous building materials: evaluation of nonisothermal moisture transport properties

Menghao Qin · Rafik Belarbi · Abdelkarim Aït-Mokhtar · Lars-Olof Nilsson

Abstract The paper presents a mathematical model for calculating the nonisothermal moisture transfer in porous building materials. The simultaneous heat and moisture transfer problem was modeled. Vapor content and temperature were chosen as principal driving potentials. The coupled equations were solved by a numerical method. An experimental methodology for determining the temperature gradient coefficient for building materials was also proposed. Both the moisture diffusion coefficient and the temperature gradient coefficient for building material were experimentally evaluated. Using the measured moisture transport coefficients, the temperature and vapor content distribution inside building materials were predicted by the new model. The results were compared with experimental data. A good agreement was obtained.

Nomenclature

C_m Specific moisture (m^3 kg^{-1})
C_p Specific heat (dry material) (J kg^{-1} K^{-1})
D_T Thermal diffusion coefficient due to the temperature gradient (kg m^{-1} K^{-1} s^{-1})
h_{lv} Heat of phase-change (J kg^{-1})
j Moisture flow (kg m^{-2} s^{-1})
k_p Permeability (m^2)

l Thickness of the specimen (m)
M_w Molar weight of water (g mol^{-1})
P_w Pore water pressure (Pa)
R Gas constant (J K^{-1} mol^{-1})
s Laplace transformation parameter
t Time (s)
T Temperature (K)
v Vapor content (kg m^{-3})
v_s Vapor content at saturation (kg m^{-3})

Greek letters

α Convective heat transfer coefficient (W m^{-2} K^{-1})
β Convective moisture transfer coefficient (m s^{-1})
γ Heat of absorption or desorption (kJ kg^{-1})
ε Thermogradient coefficient (kg m^{-3} K^{-1})
λ Thermal conductivity (W m^{-1} K^{-1})
ρ Density of the materials (dry condition) (kg m^{-3})
ρ_w Density of water (kg m^{-3})
φ Transformation function
σ Phase-change criterion
η Viscosity (kg m^{-1} s^{-1})
δ Moisture diffusion coefficient (m^2 s^{-1})
δ_v Vapor flow coefficient (m^2 s^{-1})

Subscripts

b Initial condition
i Isothermal case
l Liquid
t Nonisothermal case
v Vapor

M. Qin (✉)
National Institute of Standards and Technology, Mail stop 8633, 100 Bureau Drive, Gaithersburg, MD 20899, USA
e-mail: mqin@nist.gov

R. Belarbi · A. Aït-Mokhtar
LEPTAB, La Rochelle University, La Rochelle, France

L.-O. Nilsson
Division of Building Materials, Lund University, Lund, Sweden

Introduction

Moisture damage is one of the most important factors limiting a building's service life. High moisture level can

cause metal corrosion, wood decay, and structure deterioration. Normally, the moisture movement and heat transfer are highly coupled within building materials. The correct evaluation of these phenomena is important for accurately predicting the heat and moisture flows for thermal performance, material durability, and building energy consumption analyses. In addition, moisture accumulation will have an impact on the indoor air quality. High ambient moisture levels result in microbial growth, which may seriously affect human health and be a cause of allergy and respiratory symptoms.

For decades, many researchers have devoted their work to modeling the heat and moisture transfer in buildings. Most of the research is still carried out by using phenomenological macroscopic models, introducing heuristic laws relating thermodynamic forces to fluxes through moisture and temperature-dependent transport coefficients. In this way, one of the most used and accepted macroscopic models for studying heat and moisture transfer through porous media is the Luikov model [1] or Phillip and de Vries model [2], which use the temperature and moisture content as driving potentials. On the other hand, it is well known that there are three main difficulties using these models to calculate the nonisothermal moisture in porous materials. Firstly, the moisture content profile is discontinuous at the interface between two porous media, due to their different hygroscopic behavior. Secondly, in the classical Luikov model, the moisture diffusion coefficient and thermal diffusion coefficient are dependent on the two potentials. It is quite difficult to determine the double dependence experimentally. Thirdly, from a mathematical point of view, the highly coupled governing equations are difficult to handle.

To solve the problem of moisture content discontinuity, some authors modified the Luikov model to use other driving potentials instead of the moisture content. Pedersen [3] used the capillary pressure, but in practice, the use of capillary liquid pressure as a potential is problematic, because it is difficult to be directly measured. Künzel [4] used the relative humidity as a potential. Milly [5] and Janssen et al. [6] have also reformulated the Philip and De Vries equations for coupled heat and moisture transfer to obtain a "porous matrix potential" rather than moisture content as the independent variable. The calculation methodology employed by them is correct since it takes this discontinuity phenomenon at the interface into account. However, they have also changed the formulation of the classical Luikov equation and made it impossible to solve by analytical methods. As a more mathematical model, the Luikov equations have exact solutions in many circumstances, which can serve to evaluate the accuracy of approximate or numerical solutions. It is one of the main advantages of the model. Therefore, a logical improvement

is to choose a new proper driving potential to replace the moisture content for the Luikov equations.

In most modeling works, based on the Luikov model or the Phillip and de Vries model, for example, Crausse [7], Häupl et al. [8], Kari et al. [9], two transport coefficients (the moisture diffusion coefficient and the thermal diffusion coefficient) are used, each of them being dependent on both potentials. It is virtually impossible to determine this double dependence exactly, even with a major experimental effort, as has been shown by Da Cunha and Daian [10]. A common alternative is to introduce the temperature gradient coefficient, which is the quotient between the isothermal moisture diffusion coefficient and the thermal diffusion coefficient.

Generally, the coupled system for temperature and moisture potential can be handled by both analytical and numerical approaches, depending on the specific problem considered. Mikhailov et al. [11] have provided the analytical solutions for linear problems, based on the classical integral transform approach. Recently, Qin et al. [12] proposed an analytical solution using the Transfer Function Method. However, if the material properties of the porous material cannot be considered constant, the coupled system equations are nonlinear, and generally, are only numerically solvable.

In this paper, a dynamic mathematical model for evaluating the transient thermal and moisture transfer behavior in porous building materials is presented. Vapor content is chosen as the driving potential for the total moisture flow. A new experimental method for determining the moisture diffusivity and temperature gradient coefficient of building materials is investigated. The coupled system was solved by using the finite difference method. The computed results have been compared with experimental results to evaluate the validity of our approach.

Mathematical modeling

Moisture flow mechanisms

Traditionally, the moisture flow in porous materials can be regarded as a combination of vapor diffusion, with the vapor content as driving potential and liquid flow with the pore water pressure as potential. A description of the moisture flow j_v with the vapor content v as a potential for the vapor flow coefficient δ_v is:

$$j_v = -\delta_v \cdot \frac{\partial v}{\partial x} \tag{1}$$

The liquid flow depends on the pore water pressure gradients and the viscosity of water:

$$j_1 = -\frac{\rho_w \cdot k_p}{\eta} \cdot \frac{\partial P_w}{\partial x} \tag{2}$$

where P_w is the pore water pressure and can be expressed as:

$$P_w = \frac{RT\rho_w}{M_w} \ln \frac{v}{v_s} \tag{3}$$

k_p is the permeability, η is the viscosity, R is the gas constant, ρ_w is the density of liquid water, M_w is molar weight of water, and v_s is the vapor content at saturation.

Numerous different complicated descriptions of the total moisture flow have been used. However, since measured data are lacking for most complicated ones and the vapor flow and liquid flow usually occur in the same direction, and cannot be easily separated in an experiment, a simple description of the total moisture flow j_m in an isothermal case can be expressed according to Nilsson [13] by:

$$j_m = j_v + j_1 = -\delta_v \cdot \frac{\partial v}{\partial x} - \frac{\rho_w \cdot k_p}{\eta} \cdot \frac{\partial P_w}{\partial x} = -(\delta_v + \delta_1) \cdot \frac{\partial v}{\partial x}$$
$$= -\delta \cdot \frac{\partial v}{\partial x} \tag{4}$$

In the isothermal case, the second term in Eq. 4 can be translated into a term in vapor content by using the relationship in Eq. 3. And, δ is the equivalent total moisture diffusion coefficient.

When both moisture and temperature conditions vary, it is difficult to find one single parameter that governs the total moisture transport alone. A logical treatment is to use the temperature directly as one of the driving potentials and let it describe the change of the moisture transport when a temperature gradient is added:

$$j_m = -\delta \cdot \frac{\partial v}{\partial x} - D_T \cdot \frac{\partial T}{\partial x} = -\delta \cdot \frac{\partial v}{\partial x} - \varepsilon \cdot \delta \cdot \frac{\partial T}{\partial x} \tag{5}$$

where δ is the same as that for the isothermal case; D_T is the thermal diffusion coefficient due to the temperature gradient. The "temperature gradient coefficient" ε is the quotient between D_T and δ [1, 11, 12]. It has no physical meaning. But it is a good mathematical convenience and can be experimentally determined (see section "Evaluation of isothermal moisture transport coefficients" below). The second term on the right of the equal sign is "a correctional term" that shall take into consideration that the first term is not physically correct under a temperature gradient.

Coupled heat and moisture transfer in porous material

Governing equations

In the present study, the phase change occurring within porous materials acts as a heat source or sink, which results in the coupled relationship between moisture transfer and heat transfer. The heat of absorption or desorption is generally one of the sources or sinks as well. One-dimensional governing equations with coupled temperature and moisture for a multi-layer porous wall are considered, and the effect of the absorption or desorption heat is added. The moisture diffusivity is temperature and moisture dependent. A local thermodynamic equilibrium between the fluid and the porous matrix is assumed, and the equations are as follows:

$$\rho C_P \cdot \frac{\partial T}{\partial t} = \frac{\partial}{\partial x}\left(\lambda \frac{\partial T}{\partial x}\right) + \rho C_m (\sigma h_{lv} + \gamma) \frac{\partial v}{\partial t} \tag{6}$$

$$\rho C_m \cdot \frac{\partial v}{\partial t} = \frac{\partial}{\partial x}\left(\delta \frac{\partial v}{\partial x}\right) + \frac{\partial}{\partial x}\left(\varepsilon \delta \frac{\partial T}{\partial x}\right) \tag{7}$$

Equation 6 expresses the balance of thermal energy within the body; the last term in this equation represents the heat sources or heat sinks due to liquid-to-vapor phase change and to the adsorption or desorption process. Equation 7 expresses the balance of moisture within the medium; the last term in this equation represents the moisture source or moisture sink related to the temperature gradient. In Eq. 7, the coefficient σ is the phase-change criterion. It defines "the amount of transferable vapor in the body in relation to the total flow of vapor in the liquid" [1]. If $\sigma = 1$, moisture transfer occurs in vapor form, but if $\sigma = 0$, it takes place in liquid form. In the majority of cases the factor σ is less than unity ($0 < \sigma < 1$).

Boundary conditions

At the two sides of the whole multi-layer wall ($x = 0$ and $x = l_n$) (see Fig. 1), the mass diffusion caused by the temperature and moisture gradients affects the mass balance [12]. At the interfaces between two materials inside the wall, the distributions of temperature and vapor content are continuous. According to the above analysis, the boundary conditions can be given as follows: For $x = 0$:

$$\lambda \frac{\partial T(x,t)}{\partial x}\bigg|_{x=0} = \alpha_1 [T(0,t) - T_{a1}] \tag{8}$$

$$\delta \frac{\partial v(x,t)}{\partial x}\bigg|_{x=0} + \delta\varepsilon \frac{\partial T(x,t)}{\partial x}\bigg|_{x=0} = \beta_1 [v(0,t) - v_{a1}] \tag{9}$$

For $x = l_n$:

$$-\lambda \frac{\partial T(x,t)}{\partial x}\bigg|_{x=l_n} = \alpha_n [T(l_n,t) - T_{an}] \tag{10}$$

$$-\delta \frac{\partial v(x,t)}{\partial x}\bigg|_{x=l_n} - \delta\varepsilon \frac{\partial T(x,t)}{\partial x}\bigg|_{x=l_n} = \beta_n [v(l,t) - v_{an}] \tag{11}$$
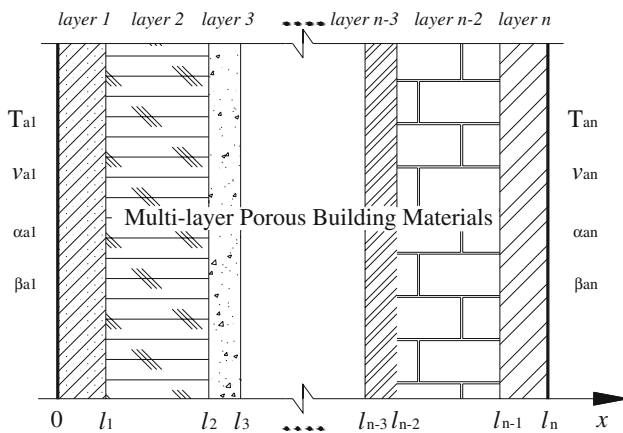
For $x = l_1, l_2, \ldots l_{n-1}$:

Fig. 1 The schematic view of the studied configuration

$$T(l_m, t) = T(l_{m+1}, t) \quad m = 1, 2, 3 \ldots n - 2 \tag{12}$$

$$v(l_m, t) = v(l_{m+1}, t) \quad m = 1, 2, 3 \ldots n - 2 \tag{13}$$

Equations 8 and 10 express the heat flux in terms of convection heat transfer at the surfaces ($x = 0$ and $x = l_n$). Equations 9 and 11 represent the moisture balance at the surfaces ($x = 0$ and $x = l_n$); the two terms on the left-hand side of the equal sign describe the supply of moisture flux under the influence of a temperature gradient and a mois-

ture gradient, respectively. The terms to the right side of the equal sign describe the amount of moisture drawn off from or into the surfaces. Equations 12 and 13 present the boundary conditions between two contacting building materials inside the wall. The initial temperature and moisture content in building material are defined:

$$T(x, 0) = T_{ini.} \tag{14}$$

$$v(x, 0) = v_{ini.} \tag{15}$$

Numerical solution

The numerical solution is based on the finite difference technique with the explicit forward differences in time. The one-dimensional process occurs along the x-axis. The material is divided into thin cells. The term of heat source (or heat sink) in Eq. 6 and the term of moisture source (or moisture sink) in Eq. 7 are treated as source terms in the discrete approximation.

The important steps of solving the coupled heat and moisture transport equations are shown in Fig. 2. The computation procedure is principally based on the calculation method presented in the flow chart. The input data comprise:

Fig. 2 Flow chart of the numerical calculation
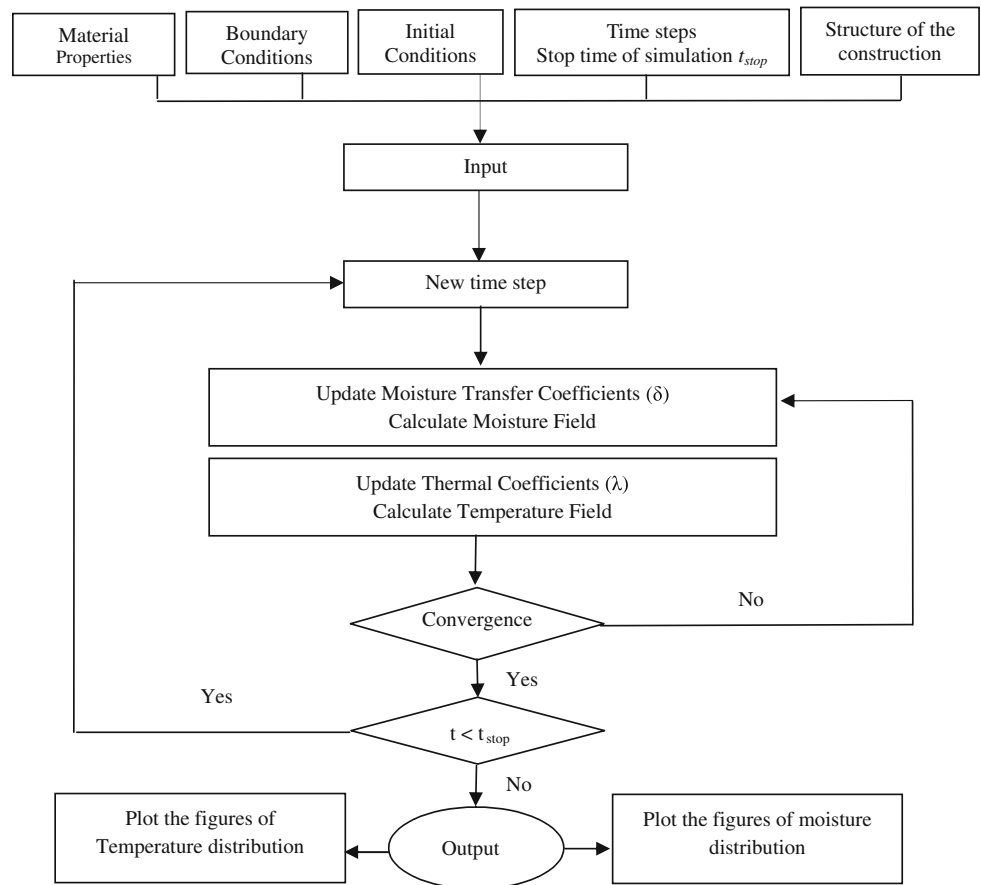
(1) The hygrothermal properties of the relevant building materials: i.e. the density, the specific heat capacity, the specific moisture capacity, the thermal conductivity, the moisture-dependent water vapor diffusion coefficient, the sorption-desorption isotherms, etc. Theoretically speaking, both sorption isotherms and moisture diffusion coefficients are moisture and temperature dependent. However, for most building materials, the temperature dependency of sorption isotherms is rather small [14]. So there is no temperature correction for the sorption isotherms in the present simulation.

(2) The climatic boundary conditions (temperature and vapor content) on the two sides exposed to the ambient air, and the heat and moisture transfer coefficients at the surfaces. The current model does not consider the radiation on the surfaces.

(3) The setting of time step, which depends on the climate condition and the required calculation accuracy.

(4) The geometrical design of the multi-layer building materials, in one-dimensional case, the mesh size of numerical grids must be adapted to the layer structure and depends on the expected moisture and temperature fields in the building component. In the range of high moisture and temperature gradients and perhaps also at layer boundaries, mesh sizes of only a few millimeters are required [14].

After compilation of the input data the transient calculations start from initial temperature and moisture conditions, which are either based on measurements or derived from steady-state calculations. The matrix equations are solved by the tridiagonal matrix algorithm (TDMA) [15], which is a simplified form of Gaussian elimination that can be used to solve tridiagonal systems of equations. At each time step, the moisture and heat transport equations are solved consecutively with a continuous update of the transport and storage coefficients until the convergence criteria are achieved [16]. To establish termination criteria for the numerical iteration, in most cases it is sufficient when the maximum change of variables in the calculation area during two successive iteration steps falls below one-thousandth of one percent in relative humidity and one-thousandth of one degree centigrade in temperature [14]. Therefore, the convergence criteria for the calculation of vapor content and temperature can be expressed as:

$$\left| v^k - v^{k-1} \right| < e_1, \quad \left| T^k - T^{k-1} \right| < e_2$$

where e is a set value. In the current research, $e_1 = 1 \times 10^{-5}$, $e_2 = 1 \times 10^{-3}$.

Determination of transfer coefficients

Evaluation of isothermal moisture transport coefficients

To calculate Eq. 7, the isothermal moisture diffusion coefficient δ should be determined experimentally.

Most methods for determining the moisture diffusion coefficient are based on the analysis of moisture profiles. In this paper, the "Slice-dry-weight" method [16] was used to measure the moisture profile and moisture flux. According to Eq. 4, δ can be evaluated from the gradient of vapor content and moisture flux.

Evaluation of the temperature gradient coefficient

As demonstrated before, it is quite difficult to determine experimentally D_T (the thermal diffusion coefficient due to the temperature gradient). So the temperature gradient coefficient ε is introduced. Using the general equations for isothermal and nonisothermal moisture flux, ε can be expressed as follows. In the equations below, the index i and t indicate isothermal and nonisothermal cases, respectively. Equation 4 can be rewritten as:

$$-j_i = \delta_i \cdot \frac{dv_i}{dx} \tag{16}$$

Equation 5 can be rewritten as:

$$-j_t = \delta_t \cdot \frac{dv_t}{dx} + \delta_t \cdot \varepsilon \cdot \frac{dT}{dx} \tag{17}$$

Further, Eqs. 17 and 16 can be written:

$$\varepsilon \cdot \frac{dT}{dx} = -\frac{j_t}{\delta_t} - \frac{dv_t}{dx} \tag{18}$$

$$\frac{1}{\delta_i} = -\frac{1}{j_i} \cdot \frac{dv_i}{dx} \bigg|_{v_i(x)=v}, \quad v_i(0) \leq v \leq v_i(l) \tag{19}$$

As mentioned in section "Moisture flow mechanisms," in the present model, the moisture diffusion coefficient δ_t in Eq. 17 is the same as the isothermal moisture coefficient δ_i used in Eq. 16. The difference between the isothermal and noisothermal cases is described by the second term on the right of the equal sign of Eq. 17, which takes into consideration that the first term is not physically correct under a temperature gradient. Insertion of Eq. 19 into Eq. 18 yields:

$$\varepsilon = \frac{1}{\frac{dT}{dx}} \cdot \left[\frac{j_t}{j_i} \cdot \frac{dv_i}{dx} \bigg|_{v_i(x)=v_t} - \frac{dv_t}{dx} \right] \tag{20}$$

This means that each point of $\frac{dv_i}{dx}$ is chosen at the same moisture content level as the corresponding, $\frac{dv_i}{dx}$ as shown in Fig. 3. The temperature gradient coefficient can thus be determined from the experimental measurements.
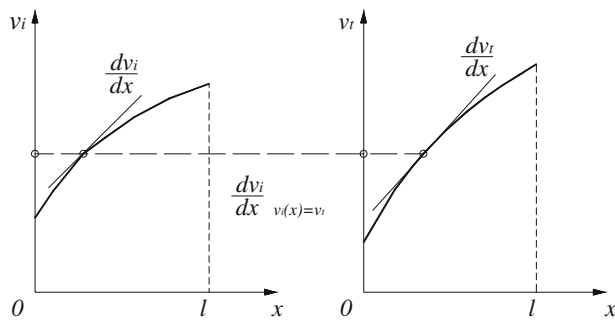
Fig. 3 Evaluation of *varepsilon* from measured data according to Eq. 20

Fig. 4 A schematic of the experimental set-up

Experimental study

Materials and preparations

Gotland sandstone [17] was used in this study. All specimens were drilled from the same piece of sandstone and have an overall dimension of 62 mm in diameter and 40 mm in length. To measure the inner moisture distribution easily, the specimen was sliced every 10 mm in length before the test. Cotton cloths were placed between interfaces of every two slices as an intermediate layer. It has been shown that the cotton cloth is a perfect intermediate that can maintain continuous moisture transfer between two materials in both hygroscopic and capillary moisture ranges [18]. The specimens were preconditioned in two ways. Half of them were saturated by storing in water for several days. The other half were oven-dried at 40 °C for several days until equilibrium was reached. Detailed data are presented in Table 1.

Tests and measurements

A modified cup method was used to measure the moisture flux and the moisture distribution of the porous building material during the nonisothermal process. The specimens were subjected not only to a moisture gradient but to a temperature gradient as well. A schematic of the experimental set-up is given in Fig. 4. Four cups with specimens were mounted into the expanded polystyrene and then placed on the steel plate. Samples were fastened with

double-sided sealant tape from IsolaPlaton® to glass cups containing salt solution. A heating device was used to supply a controlled temperature on the bottom side of the cups. The RH in the cups was controlled by different salt solutions. The whole experimental set-up was placed inside a climatic room with constant temperature and RH. Meanwhile, two other cups, functioning as reference, were put inside the climatic room without temperature gradient on both sides. Initial conditions for the experiments are listed in Table 1.

By weighing the cups regularly, the moisture loss during the experiment was measured, and then the moisture flux through the material was calculated.

During the tests, which lasted 5 weeks, temperature and relative humidity were logged in the climate room. The surface temperature and inner temperature distribution of specimens were measured with copper-constantan, bead thermocouples. The thermocouples were located at the interfaces of sandstone slices, as shown in Fig. 4.

At the end of the tests, each slice was split into two pieces. One piece was placed in the test tube that was sealed. Later the relative humidity was determined with moisture probes (at 20 °C). The other piece was weighed immediately, and then oven-dried at 105 °C for 24 h and weighed again to determine the moisture ratio. With these data, the distribution of vapor content could be obtained.

Results

The distribution of temperature, moisture ratio, and relative humidity for nonisothermal and isothermal cases at end of tests are shown in Figs. 5–9, respectively. Figure 7 shows the RH within the material on the warm side is above the ambient RH. This elevated RH is mainly due to the decrease of temperature in the specimen (as shown in Fig. 5). Using the RH distribution, the temperature distribution, and the general gas law, we can determine the vapor content distributions for both cases, which are presented in Figs. 10 and 11.

Table 1 Initial conditions for nonisothermal experiments

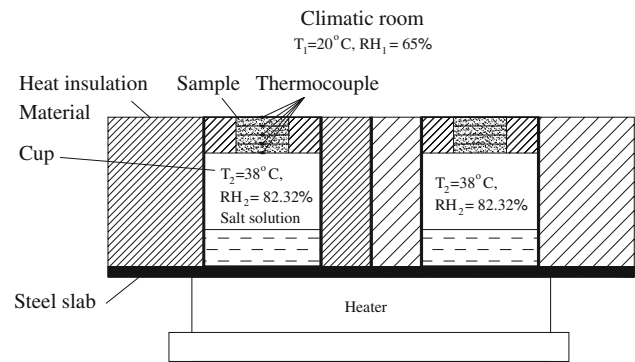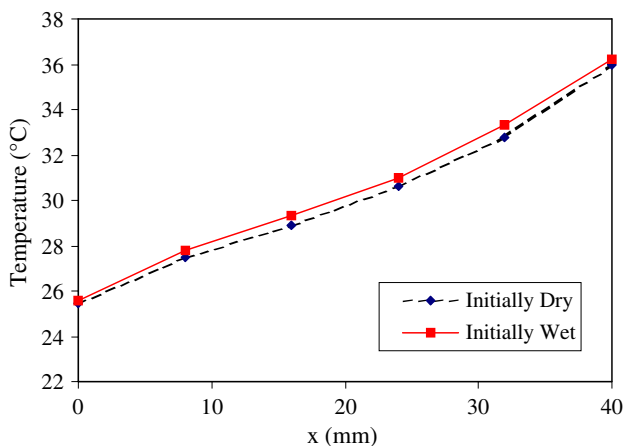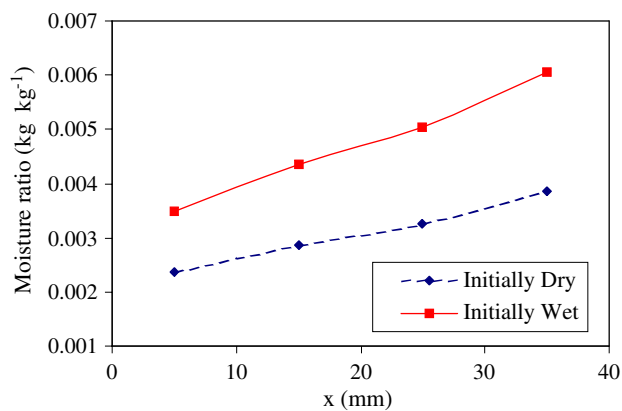|	Temperature (°C)	Relative humidity (%)
Climatic room	20 ± 1	65 ± 1.5
Specimen (initially dry)	20 ± 0.2	30 ± 1
Specimen (initially wet)	20 ± 0.2	100 ± 1
Air inside cups (at the water surface)	38 ± 0.2	82.32 ± 0.25

Fig. 5 Temperature distribution for nonisothermal case

Fig. 6 Moisture ratio distribution for nonisothermal case

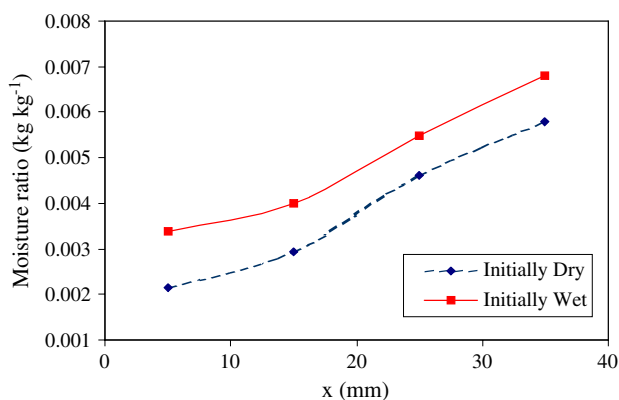Fig. 7 RH distribution for nonisothermal case

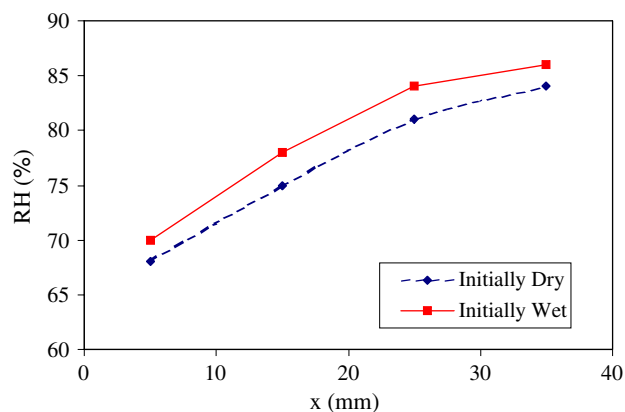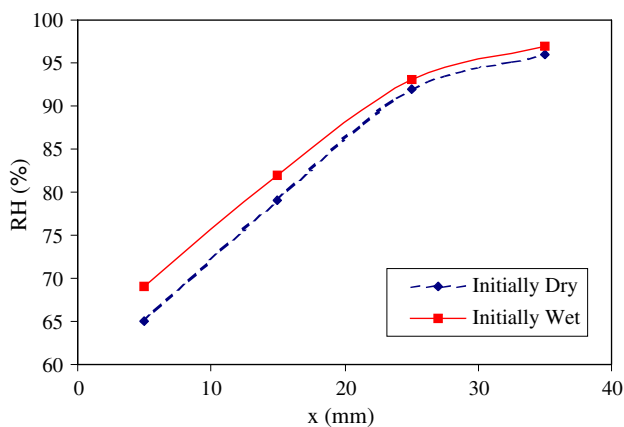Fig. 8 Moisture ratio distribution for isothermal case

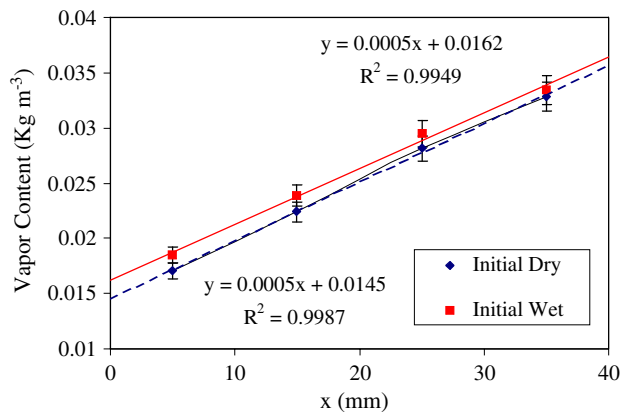Fig. 9 RH distribution for isothermal case

Fig. 10 Vapor content distribution for nonisothermal case

Since the vapor content profiles of both the nonisothermal and the isothermal cases (Figs. 10, 11) and the temperature distribution (Fig. 5) show very small curvature, in the current research, the $\frac{dv_i}{dx}$, $\frac{dv_t}{dx}$, $\frac{dT}{dx}$ can be determined as constant. Therefore, the temperature gradient coefficient can be calculated as a single average value for each case. This will greatly simplify the resolution of the coupled system, and the maximum error due to this treatment is less than 3%, which is acceptable for many engineering applications in building industry. The results of ε for both cases are presented in Table 2.
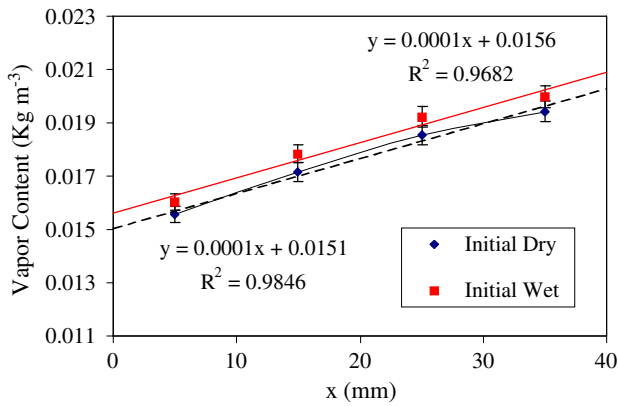
Fig. 11 Vapor content distribution for isothermal case

Table 2 Temperature gradient coefficient

	ε (% K^{-1})
Initially dry (sorption)	0.03158
Initially wet (desorption)	0.03201

Comparisons and discussion

By applying the numerical solution developed in section "Numerical solution," we can calculate the coupled heat and moisture transfer process in the specimen. All material properties of Gotland sandstone can be found in [17]. Figure 12 shows the comparison of computed temperature distribution with the experimental data. The calculated results of the present method fit the experimental data well.

Experimental and simulated distributions of vapor content are given in Fig. 13. Due to the limitation of the experimental method, we only measured the moisture distribution inside the specimens after the equilibrium (at 5 weeks). To the current graph scale, it can be seen that there is a good agreement between the computed and measured
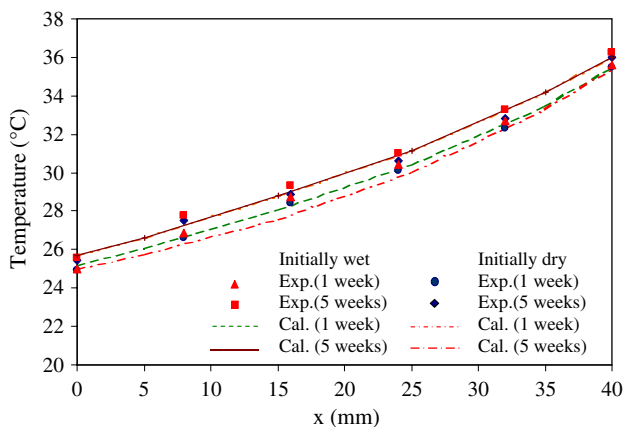

Fig. 12 Comparison of simulated temperature profile of present method with experimental data
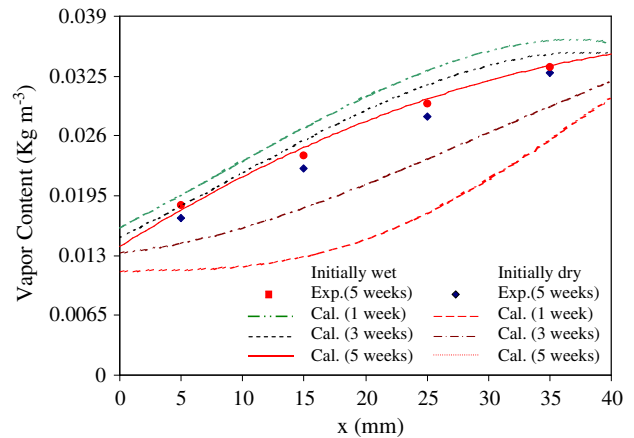

Fig. 13 Comparison of the simulated vapor content distribution with experimental data for the nonisothermal case

data. The small discrepancies between the present method and tests might be caused by using average single temperature gradient coefficient in the simulation. Nevertheless, the results still prove that the assumption of constant temperature gradient coefficient is reasonable and suitable for certain building materials in the hygroscopic moisture range with a small variation in temperature. Furthermore, the evolution of the transient moisture distribution inside the specimen during the experiment at different times was also calculated and presented in Fig. 13. We can find that the adsorption process is a little quicker than the desorption process, which highlights the adsorption hysteresis.

Conclusions

This paper proposes a mathematical model using vapor content and temperature as principal driving potentials to calculate the nonisothermal moisture transfer in the porous building materials. The coupled equations were solved by a finite difference method. A new experimental technology for determining the temperature gradient coefficient was also presented. Both moisture transfer coefficient and temperature gradient coefficient for Gotland sandstone were experimentally measured in one experiment. The calculated results have been compared with experimental data. A good agreement is obtained. Furthermore, it would be desirable to extend this modeling to multiple layers of building materials, which are more frequently used in buildings.

In the current calculation, the temperature gradient coefficient is fairly constant. The moisture dependence of this coefficient is neglected. It is necessary to note that this assumption is only validated by experiments under the specific circumstances, especially when the building material is in the hygroscopic moisture range. More work is undergoing to examine the applicability of the assumption and to validate the model in more general circumstances,

e.g., when the material is in the capillary water range and supersaturated range [16].

References

1. Luikov AW (1966) Heat and mass transfer in capillary-porous bodies. Pergamon Press, Oxford
2. Philip JR, De Vries DA (1957) Trans Am Geophys Union 38(2):222
3. Pedersen CR (1992) Build Environ 3:387. doi:10.1016/0360-1323(92)90038-Q
4. Künzel HM (1995) Simultaneous heat and moisture transport in building components: one- and two-dimensional calculation using simple parameters. IRB Verlag, Stuttgart
5. Milly PCD (1980) The coupled transport of water and heat in a vertical soil column under atmospheric excitation. Ph.D. Thesis, Massachusetts Institute of Technology, Massachusetts
6. Janssen H, Carmeliet J, Hens H (2002) J Therm Envelope Build Sci 25(4):275
7. Crausse P (1983) Etude fondamentale des transfers couplés de chaleur et d'humidité en milieu poreux non saturé. Dissertation, Institut National Polytechnique de Toulouse
8. Häupl P, Stopp H, Strangfeld P (1988) Bauzeitung 42(3):113
9. Kari B, Perrin B, Foures JC (1992) Modélisation macroscopique des transferts de chaleur et d'humidité dans des matériaux du bâtiment. Manuskript zur Veröffentlichung in RILEM, Université de Toulouse
10. Da Cunha Neto J, Daian JF (1991) Experimental analysis of moisture transport in consolidate porous media under temperature gradient. International seminar on heat and mass transfer, Dubrovnik
11. Mikhailov MD, Ozisik MN (1984) Unified analysis and solutions of heat and mass diffusion. Wiley, New York
12. Qin M, Belarbi R, Aït-Mokhtar A, Seigneurin A (2006) Int Commun Heat Mass Transfer 33(1):39. doi:10.1016/j.icheatmasstransfer.2005.08.001
13. Nilsson L-O (2004) Moisture transport in cementitious materials – theory and some experimental results. In: Knud Højgaard Conference on Advanced Cement-Based Materials – Research and Teaching, Technical University of Denmark
14. Künzel HM (1994) One and two-dimensional calculation of the simultaneous heat and moisture transport in building components, using simple parameters. Ph.D. thesis, Frauenhofer Institute for Building Physics
15. Tao WQ (1988) Numerical heat transfer (in Chinese). Xian Jiao Tong University Press, Shanxi
16. Qin M (2007) Study of the hygrothermal transfer phenomenon in building envelopes. Ph.D. thesis, University of La Rochelle, France
17. Janz M (2000) Moisture transport and fixation in porous materials at high moisture levels. Ph.D. thesis, Lund University, Sweden
18. Johansson P (2005) Water absorption in two-layer masonry systems. Ph.D. thesis, Lund University, Sweden